Available online at www.sciencedirect.com
ScienceDirect
Infrared Physics & Technology 50 (2007) 274–278
INFRARED PHYSICS & TECHNOLOGY
www.elsevier.com/locate/infrared

Effects of a p–n junction on heterojunction far infrared detectors

S.G. Matsik [a,*], M.B.M. Rinzan [a], A.G.U. Perera [a], H.H. Tan [b], C. Jagadish [b], H.C. Liu [c]

[a] Department of Physics and Astronomy, Georgia State University, Atlanta, GA 30303, USA
[b] Department of Electronic Materials Eng., Research School of Physical Science and Engineering, Australian National University, ACT0200, Australia
[c] Institute for Microstructural Sciences, National Research Council, Ottawa, Canada K1A 0R6

Available online 20 November 2006

Abstract

HEterojunction Interfacial Workfunction Internal Photoemission (HEIWIP) far infrared detectors based on the GaAs/AlGaAs material system have shown promise for operation at wavelengths up to a few hundred microns. HEIWIP detectors with GaAs emitters have been shown to operate out to 92 μm. Recent modifications to use AlGaAs emitters have extended the zero response threshold out to 128 μm. Extension to longer wavelengths will require reducing the dark current in the devices. An approach using the addition of a p–n junction in the detector, which was shown to work in QWIP and homojunction detectors is considered here. Differences between the predicted and observed threshold behavior could be explained by the presence of space charge within the device. The band bending from this space charge produces the observed variation in the threshold. The space charge can also be used to explain anomalous conduction observed at low biases. When the device is forward biased, the current is expected, to be small until the bias voltage is similar to the bandgap of 1.4 eV, above which the current should increase rapidly. Dark current was observed for biases significantly less than the bandgap. The threshold bias decreased with temperature, and was as low as 0.25 V for a temperature of 300 K. This is much lower than could be explained by thermal effects alone.

There has been extensive interest in THz detectors for applications such as security, medical diagnostics, pollution monitoring, etc. To fully exploit the advantages of THz radiation in these applications, improved detection methods are required. HEIWIP detectors have shown tailorable response thresholds out to 128 microns [1,2]. An important step in improving the detectors is the reduction of dark current so as to allow higher temperature operation. The initial homojunction detector embedded in a p–n junction had shown very low dark current (10^{-14} A for a bias field of 100 V/cm at 16 K) [3]. Hence the use of a p–n junction to reduce the dark current is a possible approach. Here, results of the insertion of a p–n junction in a HEIWIP detector are presented, and suggestions for improving the response are made.

The idea behind the inclusion of a p–n junction is that the junction can be forward biased at the threshold for current. This will restrict the dark current, while still allowing the photocurrent to pass without significant restrictions. It is also possible to use the junction to produce a LED, converting the FIR/THz photons to NIR photons which are more readily detectable. This approach has been used in QWIP detectors to produce an upconversion device [4]. A p–n junction has also been used with a device combining p and n-type quantum wells to obtain a two color device in which the response range is bias voltage selectable [5]. Here a p–n junction is included in a HEIWIP device designed for response near 1 THz with the aim of reducing the dark current.

The basic device structure consisted of 50 periods of 700 Å 3×10^{18} cm^{-3} p-doped $Al_{0.012}Ga_{0.988}As$ emitters and 2000 Å GaAs barriers. This design used a low Al fraction in the emitters to counter part of the valence band offset from doping and reduce the workfunction as has been shown previously. The top contact was 0.05 μm of 1×10^{19} cm^{-3} p-doped GaAs and the bottom contact was 1.0 μm of 5×10^{18} cm^{-3} n-doped GaAs. A partial band diagram for the structure is shown in Fig. 1.

* Corresponding author. Tel.: +1 404 6512709; fax: +1 404 6511427.
E-mail address: smatsik@gsu.edu (S.G. Matsik).

1350-4495/$ - see front matter © 2006 Elsevier B.V. All rights reserved.
doi:10.1016/j.infrared.2006.10.010

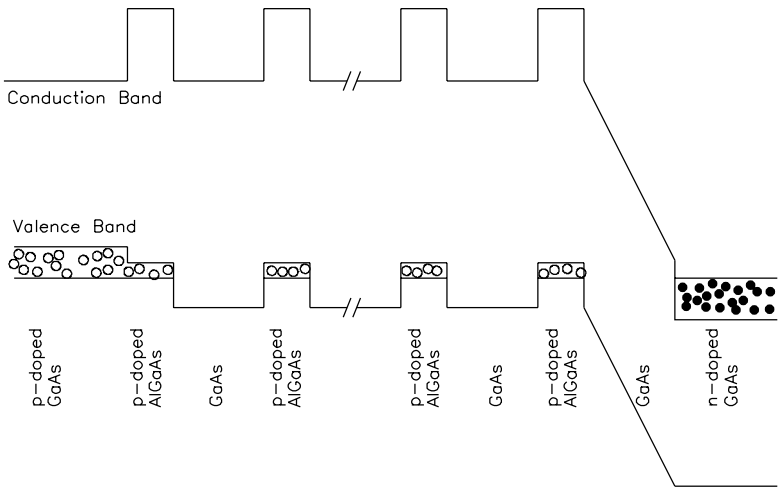

Fig. 1. The band diagram for the HEIWIP detector with the p–n junction showing the expected field distribution under forward bias. The built-in potential all drops across the last barrier. The open circles indicate holes and the filled circles electrons. Note that in this and the following band diagrams the band offsets have been exaggerated relative to the band gap to make them visible.

The response for this detector is shown in Fig. 2 at 4.2 K. The zero response threshold wavelength (λ_0) showed a strong bias dependence, increasing from 50 to 80 μm as the bias increased from 1.447 to 2.6 V (the built-in potential at this temperature was ~1.44 V). This threshold was much shorter than the expected value of ~300 μm, and the bias dependence was not expected to be as strong as was observed (an expected shift corresponding to 2–3 meV compared to the 7 meV observed).

In order to understand this behavior, the bias temperature was measured at various temperatures. Due to the space charge associated with the p–n junction, it was not possible to obtain the barrier height from an Arrhenious plot. However, the plots of dark current with temperature did provide important information for understanding the behaviour of the detector.

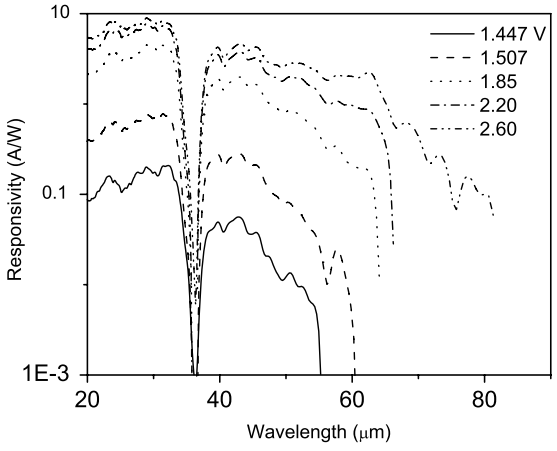

Fig. 2. The measured response for the FIR detector for various biases at 4.2 K. The built-in potential of the p–n junction is ~1.44 V at this temperature. As the bias is increased the response increases, and the threshold wavelength (indicated by where the curves stop) also increases significantly. The change in current used to define the threshold is due to the increased noise associated with reduced resistance at larger biases.

The measured dark current in the detector at 20, 77, and 300 K is shown in Fig. 3(a). The most important feature to note is the very large change in threshold voltage. The threshold was expected to correspond to the bandgap in the material which should vary from 1.4 to 1.5 eV as the temperature is varied. However, the observed threshold varied from 1.43 V at 20 K down to a minimum of 0.25 V at 300 K. This large shift was not observed in the QWIP devices, and was not expected in the present device. This discrepancy has led to the further consideration of the conditions when a p–n junction is included in an IR detector.

There are two fundamental differences between the present device, and the QWIP devices employing a p–n junction. The first is the inclusion of an LED structure in all the QWIP devices. This serves to separate the p and n doped regions when the bias is low. As a result the current at any location will consist primarily of majority carriers with only a negligible contribution from the minority carriers. The HEIWIPs have the p and n-type regions separated only by a single barrier with a thickness of 0.2 μm. This makes it easier for carriers to travel from one region to the other, and as a result there will be a significant minority carrier contribution in the HEIWIP case. The second feature is related to the design for FIR detection used in the HEIWIPs, as can be understood by considering band diagrams for the QWIP and HEIWIP structures as shown in Fig. 4. The QWIP diagram is that of a typical type I superlattice. In this, the wells for the conduction and valence bands are located in the same layer. As a result any minority carriers generated either by pair production or by transport through the structure, will be localized in the same spatial region as the majority carrier. This allows them to rapidly recombine leaving no net space charge in the region. On the other hand, the HEIWIP band diagram is similar to that of a type II superlattice. This difference is produced by the shifts of the valence band edge for the

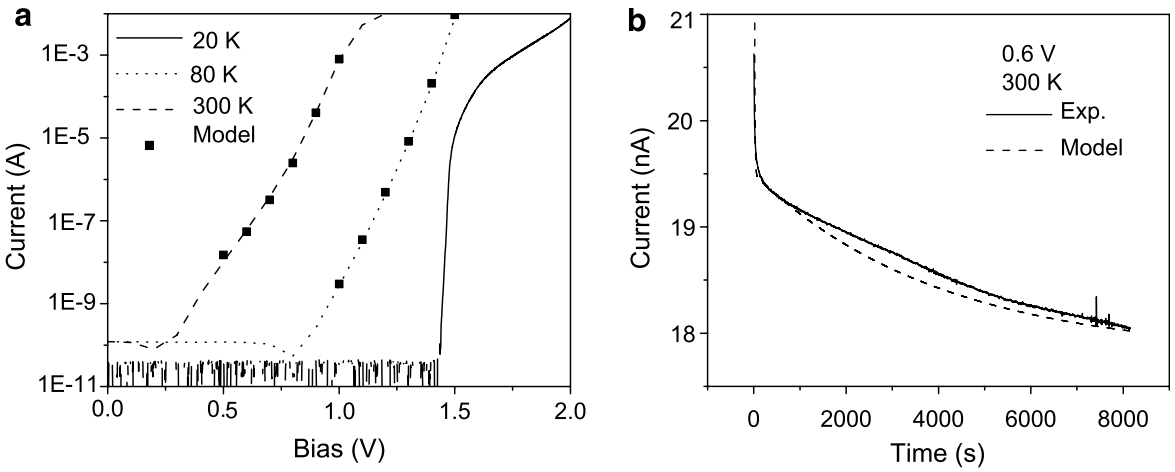

Fig. 3. (a) The dark current measured in the device at 20, 80 and 300 K showing the large change in threshold voltage for the device. (b) The transient current measured for a bias of 0.6 V at 300 K. Also shown are the modeling fits to the experimental data.

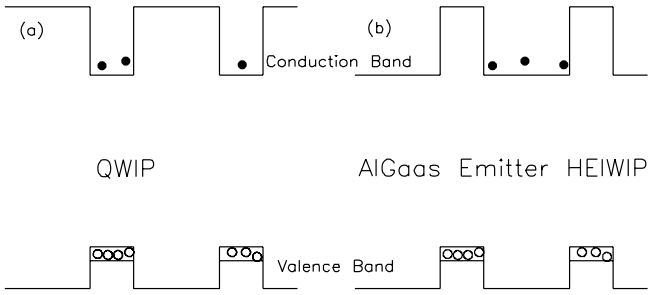

Fig. 4. A comparison of the band diagrams for (a) a standard QWIP and (b) the AlGaAs emitter HEIWIP. The fundamental difference is the well for the electrons and holes is in the same layer for the QWIP and in different layers for the HEIWIP. This leads to much less recombination in the HEIWIP than in the QWIP.

AlGaAs from the doping, and can only occur for low ($x < 0.017$) Al fraction. This means the wells for the electrons and holes are in different layers. As a result, recombination of minority carriers will be greatly slowed, and space charge can build up in the device. This space charge can then be transported to the contacts leading to a current for biases below the threshold. Supporting this idea of the buildup of space charge in the devices was the presence of a transient dark current with time scales of seconds when a bias was applied to the detector as shown in Fig. 3(b).

To verify this effect, calculations were done to model the space charge buildup in the HEIWIPs when the applied bias was zero and after bias was applied. The model will consist of two main portions: carrier generation and recombination, and carrier transport. These two parts will be solved simultaneously to obtain the space charge and current in the device. In the model the diffusion of the dopant was ignored as it should be much less than the barrier thickness.

For the generation and recombination there will be two main assumptions: (i) the generation is by thermal processes and will be independent of the location, (ii) the recombination rate will depend on the densities of both the majority and minority carriers. Based on these assumptions a model for the carrier generation and recombination at all points in the HEIWIP was developed.

For the transport of the carriers a drift diffusion model will be used at all points not on an interface between the wells and barriers. For points at the interface, drift/diffusion will be used to determine the component of the current from the barrier into the well, and thermionic emission for the component from the well into the barrier. As an additional special contribution to the current, tunneling between the n-type bottom contact and the adjacent p-type emitter will be included.

In the model the device will be divided into a sequence of segments. At each point where two segments (assumed here to be the ith and $i+1$th) meet the electric potential V_i and the electron (n_i) and hole (p_i) densities are calculated. An initial set of values for V_i, n_i, and p_i are assumed, and the model is iterated until a steady state solution is obtained. Each step of the iteration consists of three separate processes: (i) Determine the change in n_i and p_i due to generation and recombination. (ii) Determine the changes in n_i and p_i due to drift and diffusion. (iii) Determine the new values for V_i. The zero bias equilibrium distribution was obtained by starting with the assumption of no net charge in any of the layers except for the AlGaAs region closest to the n-contact. The steady state results of this calculation were then used as the initial n_i and p_i for the biased cases. A more detailed view of the model will now be presented.

The generation and recombinaton of carriers at each point was determined from

$$dn_i = (G - Rn_i p_i)dt, \quad (1)$$

$$dp_i = (G - Rp_i n_i)dt, \quad (2)$$

where G is the generation rate, R is the recombination rate, and dt is the time step. The values of G and R were first determined from the expected carrier density and carrier lifetime at equilibrium for the bulk material. The values

of G and R should not depend on the doping of the layers. It can be shown that for intrinsic matter where $n_i = p_i$ that

$$G/R = n_i^2 = \frac{1}{16}\left(\frac{2k_B T}{\pi\hbar^2}\right)^3 (m_e m_h)^{3/2} \exp(-E_g/k_B T), \quad (3)$$

where T is the device temperature, m_e and m_h are the electron and hole masses, E_g is the energy gap, k_B is Boltzmann's constant, and $\hbar$ is Planck's constant. For the barrier layers E_g is the GaAs band gap, while for the AlGaAs emitters, which are highly p-doped, it is the difference between the hole Fermi level and the conduction band. The recombination rate is given by $R = 2/\tau$ where τ is the relaxation time for the carriers.

The transport consists of two parts, drift/diffusion along the band edges, as was done previously for homojunction detectors [6], and injection at the emitter/barrier interfaces. It is assumed that the carriers generated by the thermal processes are near the band edge they will be trapped by the interfacial workfunctions. These carriers will move by drift/diffusion inside the layers, and can be injected into adjacent layers at the interfaces. The drift/diffusion contribution to the current density is calculated from

$$j_e = n\mu_e E + D_e \partial n/\partial x \quad (4)$$

for the electrons and

$$j_h = p\mu_h E + D_h \partial p/\partial x \quad (5)$$

for the holes at points on an interface. Here E is the electric field, μ is the mobility, and D is the diffusion constant. For points adjacent to an interface, the currents must be worked out separately. If the current at point i is from emitter to barrier for electrons, or from barrier to emitter for holes, the above procedure can be used with the condition any derivatives must by evaluated for a single layer using the correct endpoint formula. If the current is going in the opposite direction, then the current crossing the interface is calculated using thermal injection over the workfunction at the interface. For the emitter closest to the n-type contact there is an additional tunneling current from the emitter into the contact. The change in electron and hole densities is then given by

$$dn_i = (j_{e,i+1} - j_{e,i-1})dt, \quad (6)$$

$$dp_i = (j_{h,i+1} - j_{h,i-1})dt. \quad (7)$$

Using the electron and hole densities, the electric field distribution and the electric potential are then calculated using Poisson's equation. This completes one time step in the model. If the current is desired, it can be obtained from the values at the contacts. The above process is repeated until the current reaches a steady state value.

When the calculation was done for zero bias, it was found that for a structure with AlGaAs emitters and GaAs barriers, the spatial separation of the electrons and holes, led to a significant buildup of space charges inside the structure.These carriers then traveled through the device, and the holes collected at the emitter adjacent to the n-type contact, while the electrons were transported to the p-type contact. This process was not a single step but rather involved the carriers moving from one well into the adjacent well. When the steady state condition was used as the starting point, with the bias being turned on, it led to a slow transient behavior in the current through the device at low bias. This was particularly noticeable for room temperature measurements where a current was observed for biases as low as 0.25 V. This is caused by the thermally produced pairs being transported in opposite directions through the device by the internal fields. Because of the accumulation of space charge near the contacts, the majority of the device has a low internal electric field which will cause the carriers to move towards the contact as shown in Fig. 5. Because recombination is slow in the device, the carriers can reach the contact and be recorded as a current, even when the applied bias is less than the band gap. A fit to the steady-state current at different biases for the device at 300 K is shown in Fig. 3(a). For lower temperatures, the rate of generation of the thermal carriers is

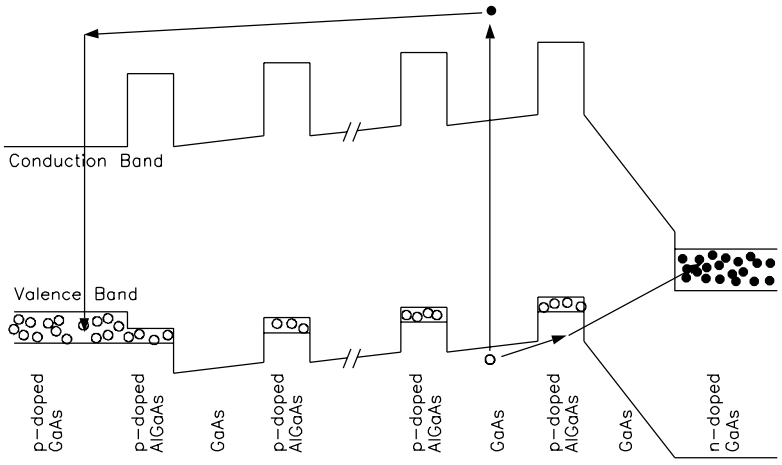

Fig. 5. The band diagram for the HEIWIP detector with the p–n junction showing the expected field distribution under forward bias. The arrows show the motion of the thermally generated electrons and holes which lead to the current for bias below the built-in voltage.

reduced, and this effect becomes smaller. For 77 K, the threshold is near the band gap, and there is a slow transient with time scales of minutes and even hours. A fit to the current vs time data is shown in Fig. 3(b). In this it is possible to identify two components in the transient response, a fast component which is caused by the escape of carrier that were trapped in the wells at zero bias, and a slow component associated with the motion of the space charge inside the device.

It is also possible to explain the reduced λ_0 value from this approach. The high doping of the n-type contact causes space charge to produce an additional barrier in the first GaAs layer. This barrier has a height of 15–25 meV depending on the bias and is responsible for the λ_0 value observed. The response being dominated by the electrons from the n-type contact is believed to be due to better transport of the electrons to the contacts in the low-field environment that is present in most of the device.

These results indicate some potential ideas for approaches to including p–n junctions into IR detectors. The first is the inclusion of a thick layer between the p and n regions of the device. The primary aim of this layer is to reduce the ability of carriers to tunnel between the regions. The modeling calculations have also shown the majority of the bias drop due to the built in voltage is across the thick layer while the applied bias is primarily across the two regions.

The second concept is to reduce the minority carrier lifetime in the device. The most obvious approach is to use designs in which the electrons and holes will be trapped in the same layer by use of a type I structure. If a type II structure is necessary, the majority carrier barriers (which serve as the minority carrier wells) should be as thin as possible to speed up the recombination of the carriers, and reduce the accumulated space charge. The inclusion of a single layer that can serve as a well for both carrier types between the p and n regions will also reduce the charge buildup. Under low bias the carriers will tend to collect in this layer and will then be able to recombine directly, reducing the space charge. This approach will be needed particularly for THz HEIWIPs which will need to use a type II structure to obtain the low barriers needed.

A potential design to take advantage of the use of a p–n junction to reduce dark current would use 300 Å GaAs emitters doped p-type to 3×10^{18} cm^{-3} and 1000 Å $Al_{0.005}Ga_{0.995}As$ undoped barriers. This will cause any thermally generated electrons to be trapped in the GaAs layers and recombine with the holes there, stopping the dark current for biases below the band gap. The device should have $\lambda_0 \sim 100$ μm. The device should have 25 emitter/barrier periods between the contacts. The top contact should be 1×10^{19} cm^{-3} p-doped GaAs and the bottom contact should be 1×10^{17} cm^{-3} n-doped GaAs. The reduced doping in the n-type bottom contact will remove the space charge induced bending near the n-type contact which produced the reduced threshold. With this design the response should be similar to that observed for GaAs emitter HEIWIPs, while by operating near the voltage threshold the dark current can be reduced by ~3 orders of magnitude. As a result the detector should operate at 77 K with a BLIP temperature of 40 K.

An alternate approach to using this in improving a design while still using the AlGaAs emitters to obtain λ_0 near 300 μm is to insert an undoped InGaAs well in the middle of each of the GaAs layers. This will serve as a recombination site for the electrons and holes. The thermally generated carriers will thus recombine before they reach the contacts, and so will not contribute to the current. However, the recombining photocarriers will still require an injected carrier to replace them, and so will contribute. The key difficulty in this approach will be designing the InGaAs wells so that the carriers will be effectively trapped in them leading to the enhanced recombination. For FIR detectors trapping will be aided by the majority of the thermally generated carriers being near the band edge. The details of the required thickness and well depth will have to be further studied to determine the optimum combination for this approach.

Acknowledgements

This work was supported in part by the US NSF under grant ECS-0553051. Australian authors acknowledge financial support from the Australian Research Council.

References

[1] S.G. Matsik, M.B.M. Rinzan, A.G.U. Perera, H.C. Liu, Z.R. Wasilewski, M. Buchanan, Cutoff tailorability of heterojunction terahertz detectors, Appl. Phys. Lett. 82 (2003) 139.
[2] M.B.M. Rinzan, A.G.U. Perera, S.G. Matsik, H.C. Liu, Z.R. Wasilewski, M. Buchanan, AlGaAs emitter/GaAs barrier terahertz detector with a 2.3 THz threshold, Appl. Phys. Lett. 86 (2005) 071112.
[3] D.D. Coon, R.P. Devaty, A.G.U. Perera, R.E. Sherriff, Interfacial work functions and extrinsic silicon infrared photocathodes, Appl. Phys. Lett. 55 (1989) 1738.
[4] E. Dupont, M. Byloos, M. Gao, M. Buchanan, C.Y. Song, Z.R. Wasilewski, H.C. Liu, Pixelless thermal imaging with integrated quantum-well infrared photodetector and light-emitting diode, IEEE Photonic Technol. Lett. 14 (2002) 182.
[5] E. Dupont, M. Gao, Z. Wasilewski, H.C. Liu, Integration of n-type and p-type quantum-well infrared photodetectors for sequential multicolor operation, Appl. Phys. Lett. 78 (2001) 2067.
[6] H.X. Yuan, A.G.U. Perera, Space-charge-limited conduction in Si n^+-i-n^+ homojunction far-infrared detectors, J. Appl. Phys. 79 (1996) 4418.